Otopro Volume xx No. x Nov 20xx pages. 85-94
P-ISSN: 1858-411x; E-ISSN: 2685-7863
DOI: 10.26740/otopro.v21n2.p85-94 https://journal.unesa.ac.id/index.php/jo
(This journal accommodates review, experimental, and thinking related to mechanical engineering and its application)

NUMERICAL INVESTIGATION OF REAR WINDSHIELD ANGLE AND REYNOLDS NUMBER EFFECTS ON THE AERODYNAMIC PERFORMANCE OF A SALOON CAR

Dwi Tarti[1], *Ika* Nurjannah[1,2*], *Herman* Sasongko[1]
[1] Department of Mechanical Engineering, Factulty of Industrial and Systems Engineering, Institut Teknologi Sepuluh Nopember, Surabaya, 60111, Indonesia
dwitarti55@gmail.com; herman@me.its.ac.id
[2]Mechanical Engineering Study program, Faculty of Engineering, Universitas Negeri Surabaya, Surabaya 60231, Indonesia
ikajannah@unesa.ac.id

Abstract. This study examined how rear windshield angle and body geometry affect the aerodynamic behavior of a saloon car model using numerical simulations. Rear windshield angles of 45°, 60°, 75°, and 90° were considered for two configurations—sharp and rounded rear corners— whereas the front windshield angle was kept constant at 30% to allow a consistent comparison. Simulations were conducted at two Reynolds numbers, 6.5×10^6 and 11.8×10^6, corresponding to inlet velocities of 22.2 m/s and 40 m/s. The simulations were performed using ANSYS Fluent 2024, focusing on the flow behavior along the upper and lower surfaces, as well as the resulting drag and lift characteristics. The results showed that increasing the rear windshield angle generally led to higher drag, mainly due to the expansion of the wake region behind the vehicle. At the same time, the lift coefficient tended to decrease as flow separation altered the pressure distribution along the body. Models with rounded corners consistently performed better than sharp-edged ones, producing lower drag and more stable flow behavior. The lowest drag coefficient (CD = 0.556) was found for the rounded configuration at a 45° rear windshield angle, whereas the highest value (CD = 0.8147) appeared in the sharp configuration at 90°. From the flow visualization, it can be seen that the sharp edges create stronger adverse pressure gradients, which trigger earlier separation and lead to a larger wake. In contrast, rounded corners helped the flow to recover more smoothly and delayed separation. At higher Reynolds numbers, the flow carries more momentum, which helps keep it attached for a longer time and reduces the wake size, ultimately lowering the drag. Overall, these findings emphasize the role of the rear windshield angle and body geometry in improving aerodynamic efficiency and minimizing energy losses.

Keywords: Rear Windshield Angle; Reynolds Number; Drag Coefficient; Lift Coefficient; Wake Flow

1 Introduction

Advances in science and technology continue to drive innovation, particularly in efforts to improve the quality of life and energy efficiency of transportation systems. In this context, fluid mechanics plays an important role in supporting engineering performance, especially in aerodynamic applications. Aerodynamic principles are widely used in the design of high-speed vehicles, such as automobiles, aircraft, and trains. Improved aerodynamic efficiency has been shown to enhances vehicle stability while reducing energy consumption, as aerodynamic drag remains a key factor influencing overall vehicle performance [1]. Therefore, reducing aerodynamic drag has become an important consideration in vehicle design, as it contributes to better performance and lower fuel or energy consumption [2], [3].

Aerodynamic optimization in vehicle design can be approached in several ways, including the use of external flow control devices, such as spoilers. These devices can improve the drag and lift characteristics by altering the flow structure around the vehicle [4]. In addition to such components, the geometry of the vehicle itself also plays a significant role in determining aerodynamic behavior. Among the different geometric parameters, the rear windshield angle is a key factor

* Corresponding author: ikajannah@unesa.ac.id

affecting the flow. Variations in this angle can affect the pressure distribution, wake size, and separation characteristics.

When the rear windshield angle is less aerodynamic, the flow tends to separate earlier, leading to a larger wake region and higher drag and lift forces. In contrast, a more streamlined configuration allows the flow to remain attached for a longer distance, resulting in a smaller wake and more stable flow pattern [5], [6], [7].

The Reynolds number, which represents the ratio of inertial to viscous forces in the flow, also plays a central role in determining the nature of flow separation and the transition from laminar to turbulent regimes [8]. At higher Reynolds numbers, the flow became more unstable and responded more strongly to adverse pressure gradients. As a result, vortex formation tends to intensify, which can increase aerodynamic drag [9], [10], [11].

Previous studies have investigated the effect of rear windshield angle on wake development. Results from numerical and experimental work on Ahmed body models show that a larger slant angle shifts the critical flow points and tends to produce a larger wake region [6].

Beyond rear geometry, factors such as ground clearance, diffuser configuration, and underbody design have been studied. For example, increasing the ground clearance generally reduces the lift, although this is often accompanied by a higher drag. Multichannel diffusers, on the other hand, can under certain conditions help stabilize the flow and reduce drag [12], [13], [14].

Vortex generators have also been investigated as a means to delay flow separation and improve lift characteristics. Even so, much of the existing work still focuses on the rear and lower parts of the vehicle, while the flow behavior over the front and upper surfaces has received comparatively less attention [15], [16].

While wake behavior downstream of a vehicle has been widely studied, relatively few studies have focused on how the rear-end geometry—particularly the rear windshield angle—affects the upstream flow near the front. The wake region can influence the incoming flow through blockage effects, which in turn modify the pressure distribution along the vehicle body. As the rear windshield angle increases, the wake tends to widen and deflect the flow upward [7], [8], reducing the flow attachment over the upper surface and lowering the surface pressure, while directing more flow toward the lower region.

These changes are closely related to variations in the drag, lift, and overall aerodynamic balance of the vehicle. At higher Reynolds numbers, the flow tends to become more sensitive to geometry-induced separation, which may further enhance the blockage effect behind the vehicle [9], [10], [11]. Although the influence of the front windshield angle has been widely reported [17], the role of rear windshield geometry in shaping upstream flow behavior and aerodynamic balance is still not fully understood

To address this gap, the present study examines the effect of rear windshield angle variations (45°, 60°, 75°, and 90°) on both upstream and downstream flow behavior of a vehicle model using 2D numerical simulations. Two Reynolds number conditions are considered (6.5×10^6 and 11.8×10^6), corresponding to inlet velocities of 22.2 m/s and 40 m/s. The front windshield angle was kept constant to ensure a consistent comparison, and simulations were conducted using ANSYS Fluent 2024.

The analysis examined the pressure distribution, wake development, and changes in drag and lift coefficients (CD and CL), focusing on how the rear geometry affected the flow ahead of the vehicle.

Overall, the results provide useful insights into the aerodynamic behavior of different configurations and can be used to support the design of more efficient vehicle geometries, particularly in relation to the rear-end shape and its interaction with the incoming flow.

2 Methodology

A two-dimensional CFD analysis using ANSYS Fluent 2024 was used to simulate the airflow around a simplified saloon car model [11], [18] [19]. The study examined four rear windshield angles—45°, 60°, 75°, and 90°—while keeping the front windshield angle fixed at 30% to ensure a consistent basis for comparison.

Simulations were conducted at two Reynolds numbers, 6.5×10^6 and 11.8×10^6, corresponding to inlet velocities of 22.2 m/s and 40 m/s [10] [9]. Two rear corner geometries, sharp and rounded, were used to assess the influence of body shape [6]. A structured mesh was applied to all configurations to maintain consistency in the numerical solution.

Because both Reynolds numbers were within the high-Reynolds-number range for external vehicle aerodynamics, the flow was classified as fully turbulent. Therefore, a turbulence model is required to accurately capture the flow separation, wake development, and pressure distribution around the vehicle body.

A uniform velocity inlet and pressure outlet were defined as the boundary conditions [20]. The aerodynamic performance was evaluated using the drag coefficient (CD), lift coefficient (CL), and pressure coefficient (CP), allowing comparison of flow behavior across the different cases [11].

To ensure the reliability of the numerical results, a validation study was conducted by comparing the baseline drag coefficient with the previously published aerodynamic data for a similar vehicle model. The detailed validation results are presented in Section 2.5 of this paper.

2.1 Preprocessing

The preprocessing stage involves geometry preparation, definition of the computational domain, mesh generation, and setup of the simulation parameters. A structured mesh is used to maintain numerical stability and to capture the boundary layer flow more accurately [21].

Since both Reynolds numbers are within the high-Reynolds-number range for external vehicle

aerodynamics, the flow was classified as fully turbulent. Therefore, the Realizable k-ε turbulence model with Non-Equilibrium Wall Functions (NWFs) was employed to capture the flow separation and wake development around the vehicle body. Air was treated as an incompressible fluid with a density of 1.225 kg/m³ and dynamic viscosity of 1.789×10^{-5} kg/m·s at 300 K. Uniform velocity inlets of 22.2 m/s and 40 m/s were applied at the inlet boundary, whereas a pressure outlet boundary condition was imposed at the outlet. The vehicle body and road surface were defined as stationary, no-slip walls. All walls were assumed hydraulically smooth, and wall roughness effects were neglected. The simulations were performed using a pressure-based steady-state solver in ANSYS Fluent 2024, and convergence was achieved when the residual values dropped below 10^{-5}, and the drag coefficient remained stable with further iterations.

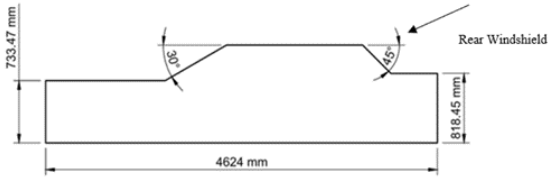

Fig. 1. 2D Desain and dimensions BMW 316i E series car model

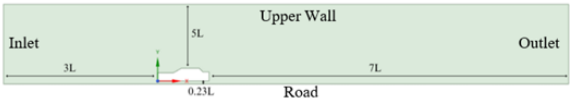

Fig. 2. 2D Domain for simulation BMW 316i E series car model

Table 1. Dimensions of the enclosure

Length between car and-	Lenght	
	Unit (L)	Unit (mm)
Inlet	3L	13872
Outlet	7L	32368
Upper Wall	5L	5755,15
Road	0,23L	271

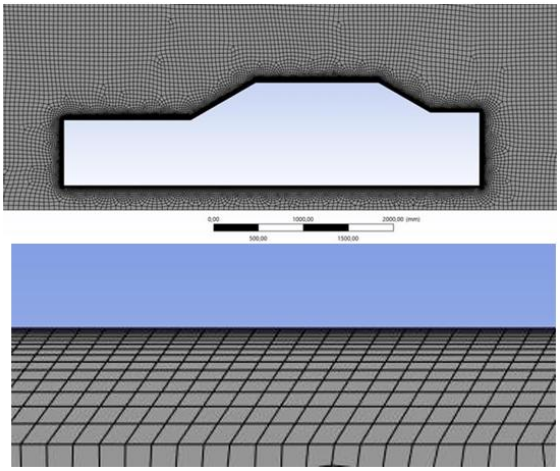

Fig. 3. Computational mesh of the vehicle model with a first-layer thickness of 1.177 mm.

2.2 Processing

The simulations were performed using a pressure-based steady-state solver in ANSYS Fluent 2024, and convergence was achieved when the residual values dropped below 10^{-5} and the drag coefficient remained stable with further iterations.

2.3 Post-processing

The post-processing stage focuses on interpreting simulation results. Velocity and pressure contours, streamlines, static pressure distributions, and velocity profiles were used to examine the flow behavior. These visualizations provide insights into how the flow develops around the vehicle and how it influences the overall aerodynamic performance.

2.4 Grid independence test

A grid independence study was performed to identify a suitable mesh configuration. Several mesh densities were tested and compared to evaluate their effect on the numerical solution. The final mesh was chosen as the smallest one that still produced negligible changes in the results [20].

Table 2. Grid independence test

Meshing	Nodes	Drag Coefficient	Eror(%)
M1	206322	0.2890140	0.00536
M2	207316	0.2890233	0.00325
M3	208340	0.2890273	0.00137
M4	208341	0.2890289	0.00054
M5	212459	0.2890290	0.00005
M6	213811	0.2890289	0.00004

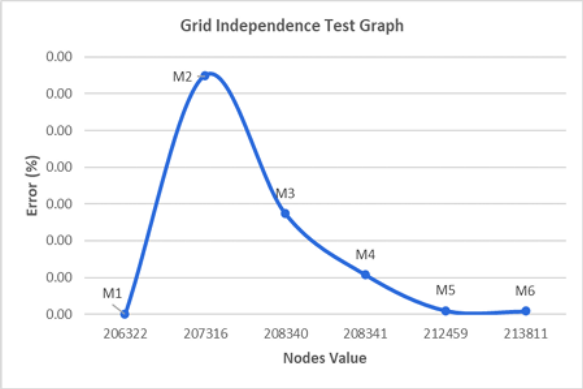

Fig.4. Grid Independence Test Graph

As shown in Table 2, the 5th mesh with 212459 nodes was used because it produced a Coefficient of Drag value of 0.2898 with an error of only 0.0005%. This very small error value indicates that the simulation results were stable and did not change noticeably even though the number of grids increased; therefore, this mesh is considered to have met the requirements of grid independence and is efficient for use in further simulations.

2.5 Validation of numerical model

To validate the numerical model, the baseline drag coefficient obtained from the grid independence test was compared with that obtained in a previous CFD [17] on a BMW 3 Series sedan model. The drag coefficient obtained in the present study was 0.2890, which is close to the reference value of 0.28714. This small difference (less than 1%) indicates good agreement with the published data and confirms that the numerical setup used in this study is sufficiently accurate for predicting the aerodynamic behavior of the saloon car model.

Table 3. Validation of Numerical Model Using Reference Study

Parameter	**Abdellah & Wang** [17]	**Present Study**
Vehicle Model	BMW 3 Series Sedan	BMW 316i E Series
CFD Software	ANSYS Fluent 17.0	ANSYS Fluent 2024
Simulation Type	3D CFD	2D CFD
Baseline Drag Coefficient (CD)	0.28714	0.2890
Reference Drag Coefficient	0.30	0.30

3 Results and discussion

3.1 Drag and left coefficient variation with Reynolds Number

The drag coefficient (CD) remains one of the main contributors to aerodynamic energy losses in road vehicles, especially at higher speeds where pressure drag becomes dominant [10], [11]. As illustrated in Figs. 5 and 6, both the Reynolds number and rear windshield angle noticeably affected the drag behavior for the sharp and rounded rear corner configurations. Across all tested cases, increasing the Reynolds number from 6.5×10^6 to 11.8×10^6 consistently led to lower drag values, suggesting stronger flow attachment and delayed separation under a higher flow momentum [6].

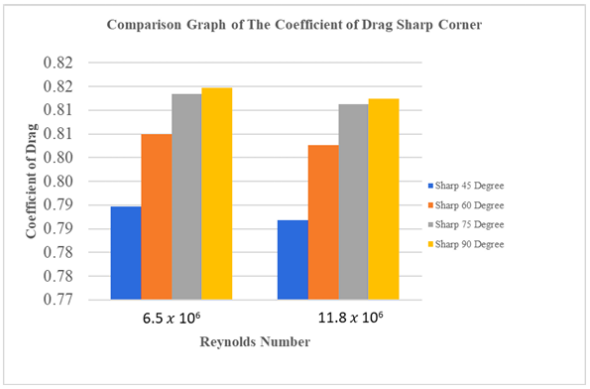

Fig. 5. Comparison graph of drag coefficient for sharp corner variation

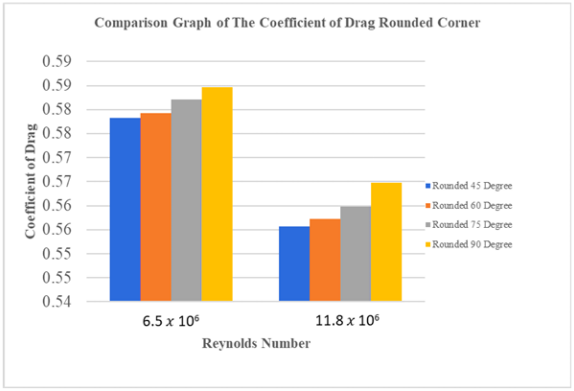

Fig. 6. Comparison graph coefficient of drag for rounded corner variation

A noticeable difference can be seen between the sharp and rounded rear corner models, with the rounded configuration generally producing lower drag than the sharp-edged case [7]. This is likely related to a more stable pressure distribution and better-controlled wake, which limits the formation of large vortical structures behind the vehicle.

As the rear windshield angle increased, the drag coefficient increased for both configurations, becoming more pronounced at 90°, where wake development became dominant. Overall, both the Reynolds number and rear-end geometry influenced the aerodynamic stability and efficiency of the vehicle.

Table 4. Comparison of drag reduction for sharp and rounded configurations

Re	Angle	C_D Sharp	C_D Rounded	Reduction (%)
6.5 x 10^6	45°	0.795	0.578	27.3
6.5 x 10^6	90°	0.8147	0.589	27.7
11.8 x 10^6	45°	0.792	0.5556	29.8
11.8 x 10^6	90°	0.812	0.565	30.4

Table 4 shows that the rounded rear-corner configuration consistently produced lower drag coefficients than the sharp-corner model for all rear windshield angles and Reynolds numbers. Overall, the rounded configuration reduced the drag coefficient by approximately 27% on average, indicating an improved aerodynamic efficiency. This reduction was associated with a smoother flow reattachment and smaller wake region behind the vehicle, which helped reduce the pressure drag.

The relationship between the drag coefficient (CD) and lift coefficient (CL) is also important for evaluating the aerodynamic stability of vehicles. Figures 7 and 8 present the lift coefficient behavior for the sharp and rounded rear-corner configurations.

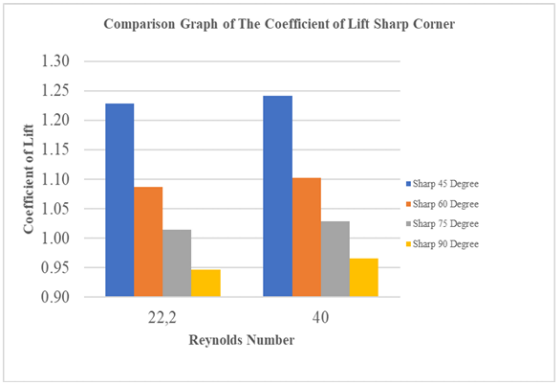

Fig. 7. Comparison graph coefficient of lift for sharp corner variations

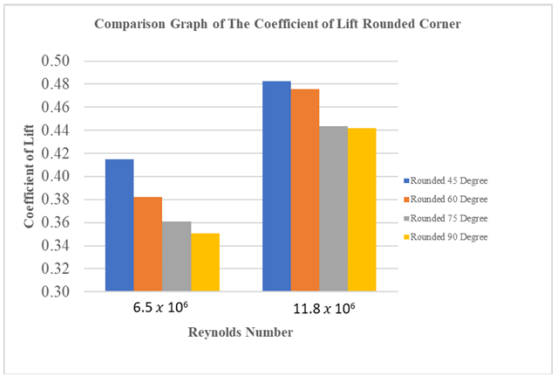

Fig.8. Comparison graph coefficient of lift for rounded corner variations

The relationship between the drag coefficient (CD) and lift coefficient (CL) is an important aspect of vehicle aerodynamic stability. Based on the results, the two rear-end configurations show different trends. In the sharp-edged case, increasing the Reynolds number tends to slightly increase the lift coefficient, which may be associated with higher uplift and reduced downforce.

While higher Reynolds numbers generally reduce the wake size in sharp-edged geometries, pressure recovery does not seem to be as effective as in the rounded configuration. This is one possible reason why the sharp rear-end models produced a higher lift than the rounded ones.

For the rounded configuration, the lift coefficient increased more noticeably with increasing Reynolds number. This behavior is related to the improved flow attachment along the vehicle surface, which creates a larger pressure difference. The highest lift coefficient was observed at a 45° rear windshield angle, reaching CL = 1.2413 at a Reynolds number of 11.8 × 10^6.

3.2 Analysis Flow Characteristics on Sharp and Rounded Corner Rear Windshield Angle 45^0

At a 45° rear windshield angle, the wake region was noticeably smaller than that at 90°. This section examines the aerodynamic behavior of sharp and rounded rear corners, focusing on the differences in pressure distribution and flow patterns and how they influence on drag.

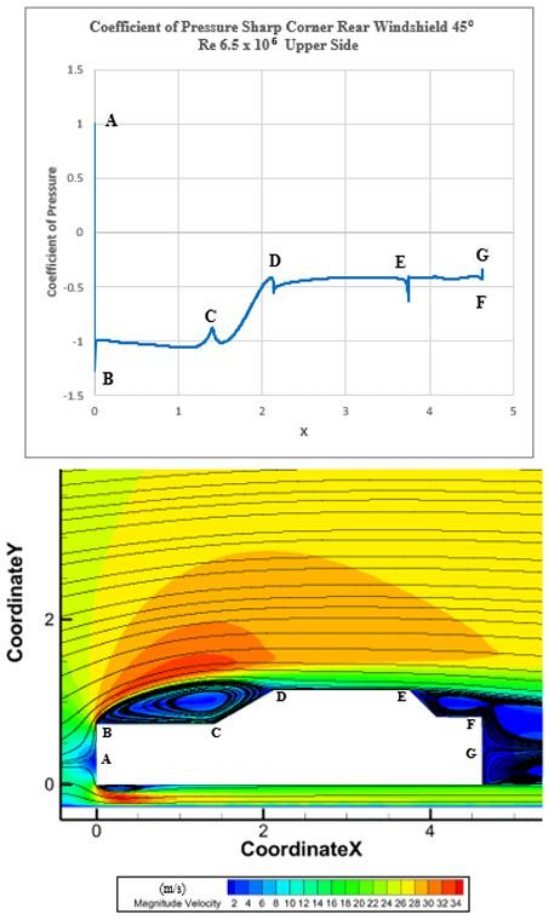

Fig. 9. Distribution of pressure coefficient (Cp) as a function of x and streamline visualization over the upper sharp corner at α = 45° and Re = 6.5 × 10^6

The pressure coefficient distribution for the model with a 45° rear windshield angle at Re = 6.5 × 10⁶ shows clear variations along the surface. Near the front region (point A), Cp approaches a value close to 1, which is consistent with a stagnation point where the incoming flow slows down significantly.

As the flow moved past this region, it accelerated around the corner (point B), causing a noticeable drop in pressure. This was followed by the onset of separation and the formation of a corner vortex. Farther downstream, point C was located within the recirculation zone behind the vehicle, where the pressure remained low, suggesting a developed wake.

Near point D, the flow starts to recover and becomes more stable, marking the transition from separation to reattachment. However, the sharp rear geometry tended to induce another separation near point E, leading to further growth of the wake region. Deeper inside the wake (point F), both the velocity and pressure remained low, indicating the presence of weak vortex-dominated flow structures.

Toward the outer edge, Cp increased gradually at point G, showing partial pressure recovery as the flow mixed with the surrounding stream. Overall, the sharp rear-end configuration led to earlier separation and a larger wake, which contributed to a higher aerodynamic drag.

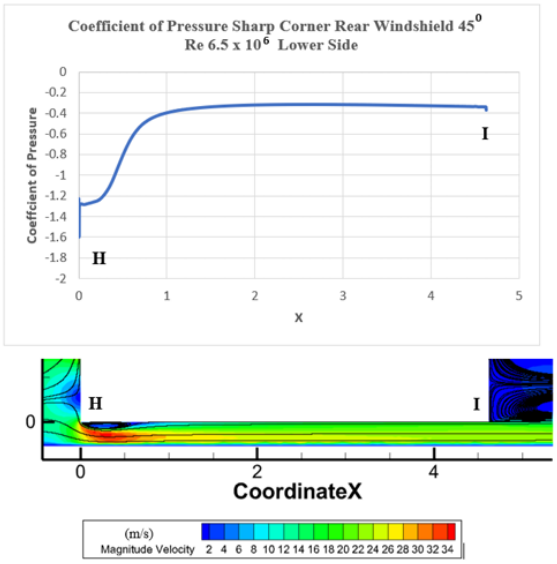

Fig. 10. Cp Distribution along the lower surface and streamline visualization for the sharp rear corner configuration (α = 45°, Re = 6.5 × 10⁶)

The flow along the lower surface shows clear signs of underbody acceleration and wake formation. Near the front underside (point H), the pressure coefficient (Cp) drops to a low value as the flow accelerated through the narrow gap between the vehicle floor and the ground. This behavior is typical of ground-effect conditions, where the confined space increases the flow velocity and reduces the static pressure [11].

As the flow moves downstream toward point I, the C_p value gradually increases. This suggests a reduction in the flow velocity and the beginning of pressure recovery. The streamline pattern revealed a recirculation region near the rear underbody. This is likely caused by the sharp geometric transition in the rear section, which makes it harder for the accelerated flow to stay attached to the surface.

The recirculation region beneath the vehicle weakens the underbody flow and increases the drag by enlarging the low-pressure zone. It also affects the lift and overall aerodynamic balance. While a narrow underbody clearance and sharp contours can strengthen the ground effect, they also make the flow more susceptible to separation and vortex formation. Because of this, the underbody geometry and pressure distribution need to be designed carefully to maintain flow stability and improve aerodynamic performance [12], [13].

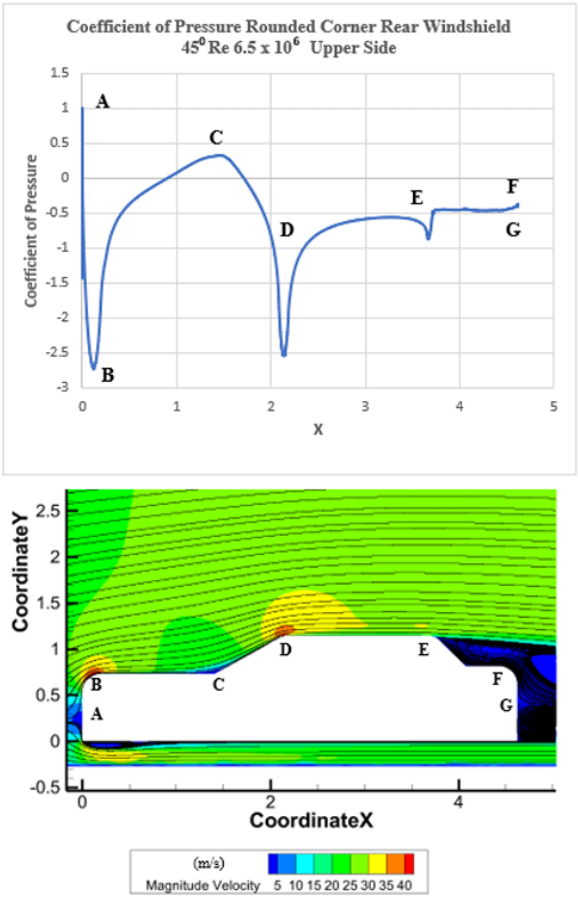

Fig. 11. Cp Distribution and streamline visualization on the upper surface for the rounded corner rear windshields (α = 45°, Re = 6.5 × 10⁶)

The Cp distribution and streamline pattern shown in Fig. 11 give a clear picture of the flow behavior along the upper surface of the model with a rounded rear corner at a 45° rear windshield angle. Near the front, Cp reached a high value, indicating a stagnation region where the incoming flow slowed down and created a local pressure peak.

Further downstream, the flow accelerated around the rounded corner, causing a drop in Cp. A small separation bubble formed in this region, but unlike the sharp-edged case, it remained limited and did not develop into a large

wake. The flow then gradually reattached, as seen from the smoother streamline pattern in Fig. 11.

In the downstream region, the pressure remained low, suggesting flow reversal and energy loss. However, the rounded geometry helped the flow recover relatively quickly, with Cp increasing again as the flow stabilized. A slight increase in Cp was also observed farther downstream, possibly linked to a minor secondary separation influenced by the downstream geometry [6].

Near the outer edge of the wake (point G), the pressure remained relatively low and the flow becomes weaker, with small vortex structures still present. This indicates that the wake was still confined to this region, with only limited suction effects.

Compared with the sharp-corner configuration, the rounded rear geometry shows a smoother pressure variation and earlier reattachment of the flow. As a result, the wake region was less intense and more stable. These characteristics are associated with a lower pressure drag and improved flow stability along the upper surface

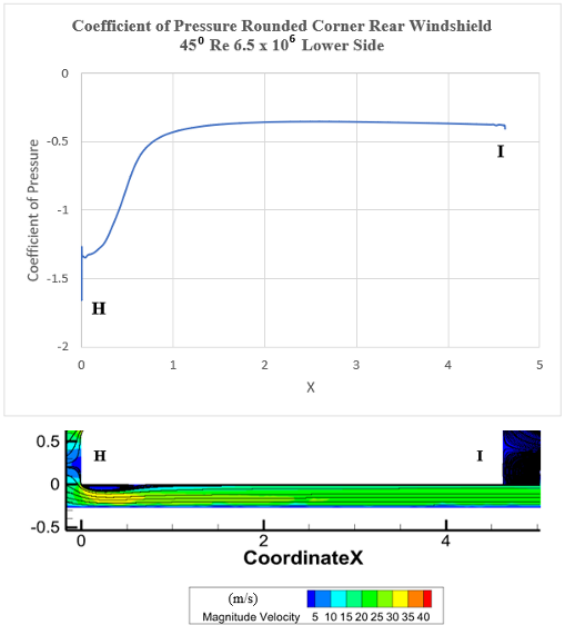

Fig. 12. Distribution of pressure coefficient (C_p) along the lower surface as a function of the streamwise coordinate, accompanied by streamline visualization for a rounded rear-corner configuration at α = 45° and Re = 6.5 × 10⁶

Figure 12 presents the Cp distribution along the lower surface and the corresponding flow pattern for the rounded rear corner at a 45° rear windshield angle. Near the front underside (point H), the flow accelerated as it entered the underbody region, causing a drop in Cp. This reduction was less pronounced than that in the sharp-corner case, indicating a smoother flow transition [7].

The streamline pattern shows that the flow remained largely attached between points H and I, with no clear indication of large vortex formation. Further downstream, Cp gradually increased as the flow slowed, indicating pressure recovery and relatively low energy loss [7], [12].

Overall, the rounded geometry supported the flow attachment along the lower surface and reduced separation [22], This led to a more uniform pressure distribution and a less developed wake region, which is consistent with the lower pressure drag and improved aerodynamic balance compared with the sharp-edged configuration.

3.3 Analysis of Flow Characteristics over Sharp and Rounded Rear Windshield Corners at 90°

At a rear windshield angle of 90°, the geometry becomes relatively blunt, which disturbs the airflow and promotes the formation of a larger wake region downstream of the body. In this section, the differences between the sharp and rounded rear corner configurations are explored, with particular attention given to how they influence the flow behavior and wake development, as well as their impact on aerodynamic drag.

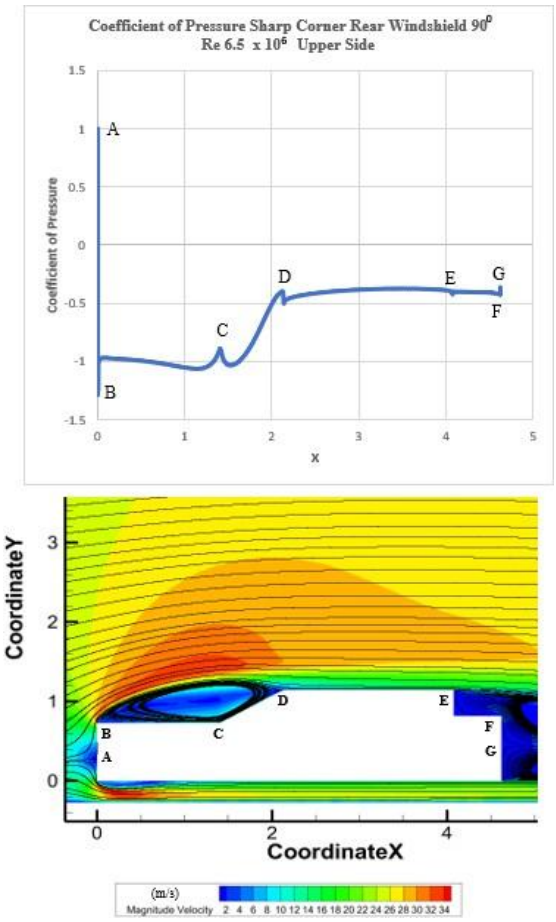

Fig. 13. Pressure coefficient (Cp) distribution along the x-direction and corresponding streamline visualization for the upper sharp-corner configuration at α = 90° and Re = 6.5 × 10⁶.

The Cp distribution and streamline pattern in Fig. 13 show that near the front region (point A), the pressure coefficient reaches a value close to 1, indicating a stagnation point where the incoming flow slows down and the pressure peaks. As the flow moved

past the leading edge toward point B, it accelerated rapidly, leading to a sharp drop in Cp and the formation of a low-pressure region. Despite this decrease, the flow remained attached to the surface, suggesting that sufficient momentum was maintained.

Further downstream, Cp began to recover but remained negative around point C, indicating gradual deceleration, whereas the flow continued to follow the surface contour. Near point D, Cp increased more noticeably as the flow began to separate after the sharp corner, marking the onset of the wake region.

At point E, Cp decreases slightly as the flow starts to stabilize within the wake, suggesting partial reattachment or adjustment to the downstream geometry. At point F, Cp drops again, reflecting low-pressure and high-velocity conditions where flow detachment and vortex formation occurred. Near point G, Cp increased slightly as the flow slowed within the wake region dominated by vortices.

Overall, Fig. 13 indicates that at a rear windshield angle of 90°, the wake becomes more pronounced, leading to a stronger separation and increased aerodynamic drag.

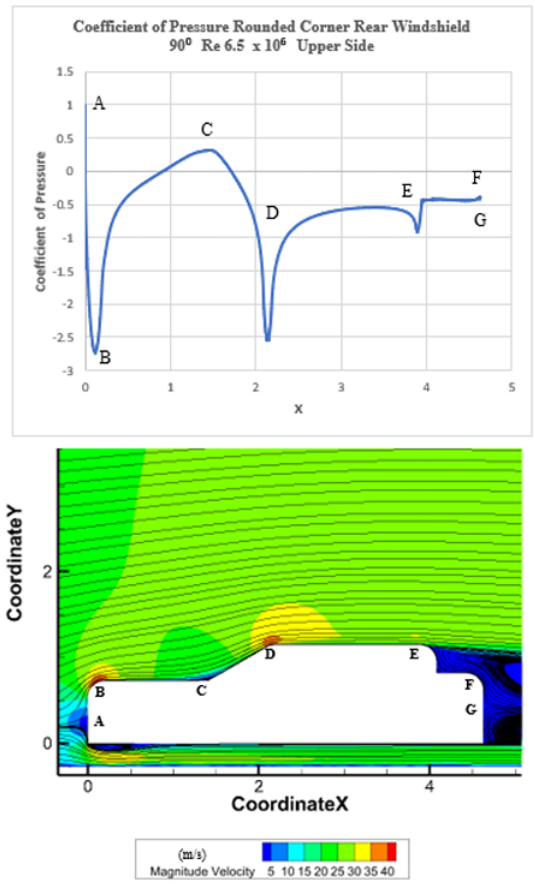

Fig. 14. Pressure coefficient (Cp) distribution along the x-direction and streamline visualization for the lower sharp corner configuration at α = 90° and Re = 6.5 × 10⁶

Fig. 14 shows the distribution of the pressure coefficient (Cp) and flow velocity along the lower surface of the vehicle for the sharp 90° front geometry at a velocity of 22.2 m/s. At point H, Cp reaches a minimum value as the flow accelerates rapidly through the sharp geometric transition beneath the vehicle. This acceleration led to flow separation and vortex formation, as indicated by the closely spaced streamlines and red–yellow velocity contours.

Moving downstream toward point I, Cp gradually increased, indicating pressure recovery as the flow slowed down. Two vortical structures were observed: a larger vortex near point H and a smaller one near point I. These vortices formed a recirculation region with low velocity, especially beneath point I, as shown by the dark blue contour.

Overall, low Cp values were linked to high-speed separated flow at sharp geometric transitions, whereas increasing Cp reflected flow deceleration and partial reattachment. The sharp front geometry promoted stronger separation and vortex formation, leading to higher aerodynamic drag.

This suggests that a smoother and more refined underbody design can help reduce separation, limit vortex formation, and improve aerodynamic performance.

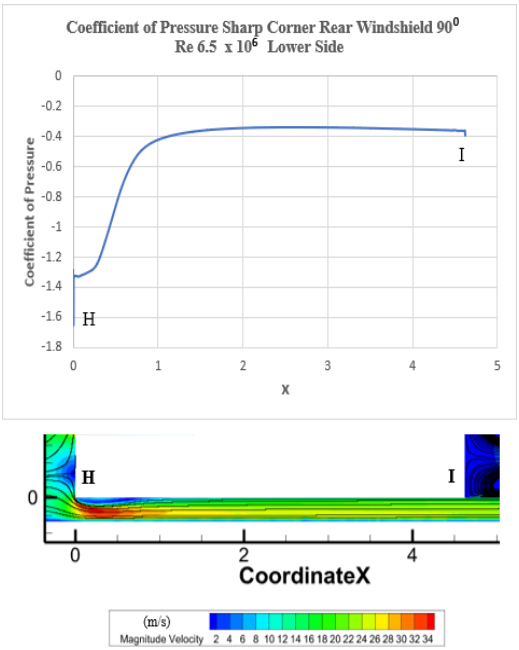

Fig. 15. Pressure coefficient (Cp) distribution along the x-direction and streamline visualization for the upper rounded corner configuration at α = 90° and Re = 6.5 × 10⁶.

Fig. 15 shows the distribution of the pressure coefficient (Cp) and the corresponding flow pattern for the sharp rear corner at a rear windshield angle of 90°. Near point A, Cp reaches a value close to 1, indicating a stagnation region where the incoming flow slows and the pressure reaches its maximum. Moving toward point B, Cp decreased sharply as the flow accelerated along the surface under a favorable pressure gradient. Beyond this point, the flow is subjected to an adverse pressure gradient and begins to lose momentum.

Near point C, the flow noticeably slows down as the pressure rises and separation begins, with diverging streamlines and the formation of a recirculation region. At point D, Cp reaches a highly negative value due to strong local acceleration caused by abrupt geometric changes. The dense streamline pattern in this region

reflected high kinetic energy, which could have led to early flow separation.

Further downstream, Cp increased again near point E as the flow slowed, indicating pressure recovery. However, the available momentum is insufficient to maintain attachment, and the flow separates, forming a strong vortex that contributes to a higher aerodynamic drag. At point F, Cp continued to increase as the flow became fully detached from the rear surface. Near point G, located within the wake region, both Cp and velocity remained low due to vortex-induced suction.

Overall, the wake region is dominated by low-pressure turbulent flow, which contributes to increased aerodynamic drag.

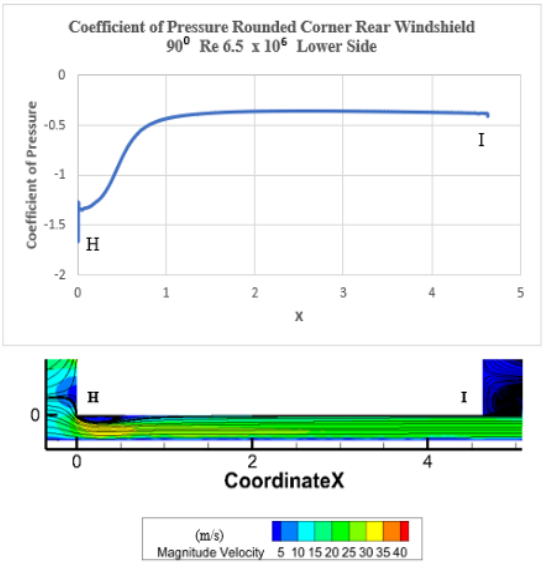

Fig. 16. Pressure coefficient (Cp) distribution along the x-direction and streamline visualization for the lower rounded corner configuration at $\alpha = 90°$ and $Re = 6.5 \times 10^6$

Fig. 16 shows the distribution of the pressure coefficient (Cp) and the corresponding flow pattern for the sharp rear corner at a rear windshield angle of 90°. Near point A, Cp reaches a value close to 1, indicating a stagnation region where the incoming flow slows and the pressure reaches its maximum. Moving toward point B, Cp decreased sharply as the flow accelerated along the surface under a favorable pressure gradient. Further downstream, the flow experiences an adverse pressure gradient and gradually loses momentum.

Near point C, the flow slows down more noticeably as the pressure rises and separation begins, with diverging streamlines and the formation of a recirculation region. At point D, Cp reaches a highly negative value due to the strong local acceleration caused by abrupt geometric changes. The dense streamline pattern in this region reflects high kinetic energy, which can lead to early flow separation.

Further downstream, Cp increased again near point E as the flow slowed, indicating pressure recovery. However, the available momentum is insufficient to maintain attachment, and the flow separates, forming a strong vortex that contributes to a higher aerodynamic drag. At point F, Cp continued to increase as the flow became fully detached from the rear surface. Near point G, located within the wake region, both Cp and velocity remained low due to vortex-induced suction.

Overall, the wake region was dominated by a low-pressure turbulent flow, which played a significant role in increasing the aerodynamic drag.

4 Conclusion

This study looks at the aerodynamic behavior of saloon car models with different rear windshield angles and corner geometries (sharp and rounded). The results show a clear trend: increasing the rear windshield angle led to higher drag and lower lift, regardless of the corner shape. Across all cases, the rounded configurations consistently produced lower drag and lift than the sharp-edged ones. On average, the rounded corners reduced the drag coefficient by about 27%. Higher Reynolds numbers also reduced the drag while slightly increasing the lift.

The flow field supports these findings. Larger rear windshield angles produced a more developed wake, whereas rounded corners, along with a downstream shift in separation, helped maintain a smaller wake and reduce drag.

Acknowledgement

The author would like to thank the Department of Mechanical Engineering, Sepuluh Nopember Institute of Technology, and all parties who have supported this research. It is hoped that this work will be useful to readers and serve as a reference for future studies.

References

[1] R. Pratama, “Pengaruh Desain Aerodinamika Terhadap Efisiensi Bahan Bakar pada Kendaraan Bermotor Listrik,” vol. 1, no. 2, 2025.

[2] A. W. Huluka and C. H. Kim, “Numerical study on aerodynamic drag reduction and energy harvest for electric vehicle: a concept to extend driving range,” *IOP Conf. Ser.: Mater. Sci. Eng.*, vol. 700, no. 1, p. 012009, Nov. 2019, doi: 10.1088/1757-899X/700/1/012009.

[3] M. G. Connolly, A. Ivankovic, and M. J. O’Rourke, “Drag reduction technology and devices for road vehicles - A comprehensive review,” *Heliyon*, vol. 10, no. 13, p. e33757, Jul. 2024, doi: 10.1016/j.heliyon.2024.e33757.

[4] M. M. Islam and M. I. Inam, “Numerical Investigation of the Effect of Different Airfoil Profile of a Spoiler in a Car,” *SCS:Engineering*, vol. 1, pp. 6–11, May 2025, doi: 10.38032/scse.2025.1.2.

[5] A. Ali Wafa and H. Sasongko, “Studi eksperimen dan numerik karakteristik aliran dua dimensi pada

thick plate–rounded leading edge (r/t = 0,2) dengan pengaruh Reynolds number (Ret = $6{,}76\times10^4$ dan Ret = $10{,}15\times10^4$) dan panjang aksial (c/t = 6,5 dan c/t = 10).," *JURNAL TEKNIK ITS*, vol. Vol. 9, No. 2, p. 2020.

[6] T. Tunay, B. Sahin, and V. Ozbolat, "Effects of rear slant angles on the flow characteristics of Ahmed body," *Experimental Thermal and Fluid Science*, vol. 57, pp. 165–176, Sep. 2014, doi: 10.1016/j.expthermflusci.2014.04.016.

[7] H. Bao, C. Wang, and Y. Wu, "Effects of Rear Window Angle on Car Aerodynamic Characteristics," presented at the 2020 3rd World Conference on Mechanical Engineering and Intelligent Manufacturing (WCMEIM), Shanghai, China, 2020. doi: 10.1109/WCMEIM52463.2020.00141.

[8] S. H. S.P, W. A. Widodo, B. Junipitoyo, W. Suryono, and S. Supriadi, "Investigasi Perbandingan Posisi Rectangular Flat Plate Vortex Generator dengan Posisi Straight pada Wing Airfoil NACA 43018," *jp*, vol. 3, no. 3, pp. 36–43, Sep. 2018, doi: 10.46491/jp.v3e3.43.36-43.

[9] Fox, R. W., & McDonald, A. T, *Introduction to Fluid Mechanics*. Wiley., 1998.

[10] Hucho, W, *Aerodynamics of Road Vehicles*. 1997.

[11] Anderson, J. D, *Fundamentals of Aerodynamics.* McGraw-Hill, 2007.

[12] D. Mitra, "Design Optimization of Ground Clearance of Domestic Cars," *International Journal of Engineering Science and Technology*, vol. 2, 2010.

[13] I. Siregar, "Studi Eksperimen Pengaruh Variasi Ketinggian Ground Clearance dengan Four-Channel Diffusers pada Bagian Belakang Bodi Bus," Master's thesis, Institut Teknologi Sepuluh Nopember, Surabaya, Indonesia, 2016. [Online]. Available: http://repository.its.ac.id/id/eprint/75927

[14] I. M. B. P. Dewa, "Analysis of Airflow Patterns and Pressure Distribution Characteristics on Cars with Variations of Under Front End Tilt Angle," *Natural Sciences Engineering and Technology Journal*, vol. 3, no. 2, pp. 248–258, 2023, doi: 10.37275/nasetjournal.v3i2.42.

[15] A. Seshagiri, E. Cooper, and L. W. Traub, "Effects of Vortex Generators on an Airfoil at Low Reynolds Numbers," *Journal of Aircraft*, vol. 46, no. 1, pp. 116–122, 2009, doi: 10.2514/1.36241.

[16] P. N. Selvaraju, D. K. M. Parammasivam, and D. G. Devaradjane, "ANALYSIS OF DRAG AND LIFT PERFORMANCE IN SEDAN CAR MODEL USING CFD".

[17] E. Abdellah and B. Wang, "CFD analysis on effect of front windshield angle on aerodynamic drag," *IOP Conf. Ser.: Mater. Sci. Eng.*, vol. 231, p. 012173, Sep. 2017, doi: 10.1088/1757-899X/231/1/012173.

[18] K. H. Versteeg and Malalasekera, *An Introduction to Computational Fluid Dynamics: The Finite Volume Method*, 2nd ed. Harlow, England: Pearson Education Limited, 2007.

[19] A. Yaqin, A. Z. Hudaya, and R. Wibowo, "Simulasi Aliran Dua Fasa Stratified Air–Udara pada Pipa Horizontal," *Journal of Industrial Engineering and Technology*, vol. 5, no. 1, pp. 98–107, 2024, doi: 10.24176/jointech.v5i1.13492.

[20] ANSYS Inc., "ANSYS Fluent Theory Guide," ANSYS Inc., Canonsburg, PA, USA, 2024. Accessed: Jan. 25, 2026. [Online]. Available: https://www.ansys.com/products/fluids/ansys-fluent

[21] I. Sadrehaghighi, "Structure Meshing for CFD," Independent Technical Report, No. 2.20, 2023.

[22] L. L. Pauley, "A Numerical Study of Unsteady Laminar Boundary Layer Separation," PhD dissertation, Stanford University, Stanford, CA, USA, 1988. [Online]. Available: https://searchworks.stanford.edu/view/1806942.04.024